TIME HISTORY RESPONSE PREDICTION FOR MULTI-STORY BUILDINGS CONSISTING OF MIXED SOFT AND RIGID STORIES UNDER EARTHQUAKE MOTIONS

Tomofusa Akita[1] and Hiroshi Kuramoto[2]

[1] *Assistant Professor, Dept. of Architecture, Chiba University, Chiba, Japan*
[2] *Professor, Dept. of Architectural Engineering, Osaka University, Suita,Japan*
Email: akita@faculty.chiba-u.jp, kuramoto@arch.eng.osaka-u.ac.jp

ABSTRACT :

The purpose of this research is to take into account the higher mode responses in evaluating the responses of the multi-story irregular-shaped buildings consisting of mixed soft and rigid stories in which the story collapse mechanism is formed under earthquake motions. In previous study, one of the authors has proposed a method for evaluating the time history responses including higher mode components of the inter-story shear and drift for multi-story regular-shaped buildings. The results indicated that the time history response of the buildings can be accurately predicted by the proposed method. However, the applicability of the proposed method for multi-story irregular-shaped buildings is not confirmed yet. Therefore, the applicability of the proposed method for the irregular-shaped buildings was investigated in this paper. The modified method using the equivalent participation vector of the dominant higher mode for evaluating the time history responses of the inter-story shear and drift is proposed. The results showed that the predicted the time history responses of the inter-story shear and drift by the modified method has good agreement with the time history analysis result.

KEYWORDS: Buildings with story collapse mechanism, Evaluation of time history response, Higher mode responses, Equivalent mass ratio, Equivalent participation vector

1. INTRODUCTION

In Calculation of Response and Limit Strength (CRLS) implemented in June 2000 in accordance with the Building Standard Law of Japan (June 1998), Capacity Spectrum Method (CSM; Freeman, 1978), based on the equivalent linearization method (Shibata, 1976), has been adopted for calculating a building's earthquake response. In this evaluation, multi-story building is necessarily reduced to equivalent single degree of freedom (ESDOF) system. However, the evaluation based on an ESDOF system cannot consider the higher mode responses in evaluating the response of the multi-story buildings. Thus, a key issue for improving the estimation accuracy by CRLS is on how to consider the higher mode responses in evaluating the response of the multi-story buildings.

The method of the considering the higher mode responses about multi-story pure frame building was proposed and its appropriateness was examined by one of the authors in previous studies (Kuramoto, 2006 and 2007). However, buildings which were dealt with in the previous studies had regular-shaped elevation. The evaluation of the higher mode responses of irregular-shaped buildings, buildings with story collapse mechanism for instance, has been not examined. In the previous study, one of the authors has proposed a method for evaluating the time history responses including higher mode components of inter-story shear and drift for multi-story regular-shaped buildings as shown in Eqn. (1) and Eqn. (2). These equations predict the time history responses accurately.

$$Q_i(t)=\sum_{j=i}^{N} m_j\left\{\sum_{s=1}^{2}{}_s\beta\cdot{}_s u_j\cdot{}_s S_a(t)-\left(1-\sum_{s=1}^{2}{}_s\beta\cdot{}_s u_j\right)\cdot\ddot{x}_0(t)\right\} \tag{1}$$

$${}_{st}\delta_i(t)={}_1\beta\left({}_1u_i-{}_1u_{i-1}\right){}_1\Delta(t)+{}_h\beta\left({}_hu_i-{}_hu_{i-1}\right)\frac{\sum_{s=2}^{3}{}_s\overline{M}\cdot{}_s\Delta(t)+{}_1\overline{M}_e\cdot{}_1\Delta_e(t)-{}_1\overline{M}\cdot{}_1\Delta(t)}{{}_2\overline{M}+{}_1\overline{M}_e-{}_1\overline{M}} \tag{2}$$

$${}_1u_0={}_hu_0=0 \tag{3}$$

$${}_h\beta\cdot{}_hu_i={}_2\beta\cdot{}_2u_i+{}_1\beta_e\cdot{}_1u_{ei}-{}_1\beta\cdot{}_1u_i \tag{4}$$

Where m_i is the i th story mass, ${}_1\overline{M}$, ${}_1\overline{M}_e$, ${}_2\overline{M}$ and ${}_3\overline{M}$ are the equivalent mass for the first mode, the elastic first mode, the elastic second mode and the elastic third mode respectively, ${}_sS_a(t)$ is the spectral acceleration for s th mode at time t, $\ddot{x}_0(t)$ is the acceleration of the input ground motion at time t, ${}_1\beta\cdot{}_1u_i$, ${}_1\beta_e\cdot{}_1u_{ei}$ and ${}_2\beta\cdot{}_2u_i$ are the participation vector for the first mode, the elastic first mode and the elastic second mode respectively, ${}_1\Delta(t)$, ${}_1\Delta_e(t)$, ${}_2\Delta(t)$ and ${}_3\Delta(t)$ are the representative displacement for the first mode at time t, the elastic first mode at time t, the second mode at time t and the third mode at time t respectively.

The purpose of this research is to take into account the higher mode responses in evaluating the responses of the multi-story irregular-shaped buildings consisting of mixed soft and rigid stories in which the story collapse mechanism is formed under earthquake motions. In this paper, the applicability of the Eqn. (1) and Eqn. (2) for the irregular-shaped buildings was investigated first. The time history responses evaluation of the inter-story shear and drift were conducted using the Eqn. (1) and Eqn. (2) on four irregular-shaped buildings with different soft story location and one wall-frame building with soft middle-story. Then the evaluation method for the buildings with story collapse mechanism was proposed based on the examination of the characteristics of seismic response of the irregular-shaped building.

2. OUTLINE OF THE ANALYZED BUILDINGS

Figure 1 shows the plan and elevation of the analyzed buildings. 14-story frames have the plan with 1 span of 10.8m at the transverse direction and 6 spans of 7.2m at the longitudinal direction. 14F01 (Fig. 1(a)) has the soft story at the first story, 14F03 (Fig. 1(b)) has it at the third story, 14F07 (Fig. 1(c)) has it at the seventh story and 14F12 (Fig. 1(d)) has it at the twelfth story. 12F06 (Fig. 1(e)) is the building in which shear walls were added at the center span except for the sixth story to the building analyzed in the previous study (Kuramoto, 2006). Tables 1(a) and 1(b) show the details of the columns section and the shear walls section of 14-story buildings. 14F01, 14F03, 14F07 and 14F12 are the buildings in which the shear walls indicated in Table 1(a) were replaced by the columns indicated in Table 1(b). Tables 1(c), 1(d) and 1(e) show the columns, shear walls and beams section of 12-story building. In this paper, the story only composed by the columns is defined as soft story, while the story with shear walls is defined as the rigid story. Mode adaptive pushover analysis (MAP analysis; Kuramoto and Matsumoto, 2004) and time history earthquake response analysis were carried out on each building.

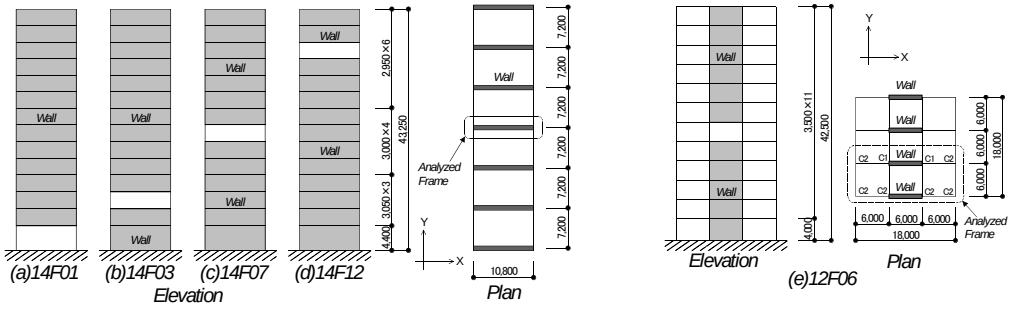

Figure 1 Analyzed buildings

For the time history response analysis, the El Centro NS (1940) earthquake record was used as input ground motion. The input ground motions scaled to a maximum velocity of 25cm/sec (El25), 50cm/sec (El50) and 75cm/sec (El75) were inputted to each building respectively. Furthermore, the input ground motion scaled to a maximum velocity of 100cm/sec (El100) was only inputted to 14F07. The end spring model using the Takeda model (Takeda et al., 1970) for its hysteresis characteristics was applied to beams, and the multi spring model (MS model; Gu, Inoue and shibata, 1998) was applied to columns and shear walls. Shear springs with the stiffness degradation due to shear cracks were set in the center of the columns and shear walls. However, the shear yielding was not considered in the shear springs. Viscous damping for the analysis is proportional to the instantaneous stiffness and is assumed to have a 5% damping coefficient with respect to the elastic first mode period. The Newmark-β method ($\beta = 1/4$) was used for the numerical integration. The duration of input ground motion was 15 seconds, and the time intervals of integral were set to 0.0001 seconds for 14-story buildings and 0.004 seconds for 12-story building respectively.

Table 1 Section of the members

(a) Columns and walls section of 14-story buildings

floor	Fc (N/mm²)	column				wall	
		section	longitudinal bar		hoop	thickness	longitudinal and transvese bar
			X-dir	Y-dir			
9F-14F	27	900×1050	5-D29	2-D29, 3-D16	8-D10@200	150	D10@150Single
6F-8F	27	1000×1050	7-D29	2-D29, 3-D16	6-D13@200	180	D10@200Double
5F	30	1000×1050	7-D29	2-D29, 3-D16	6-D13@200	180	D10@200Double
3F,4F	30	1050×1050	10-D29	2-D29, 3-D19	8-D13@200	200	D10@150Double
1F,2F	33	1050×1050	10-D29	2-D29, 3-D19	8-D13@200	200	D10@150Double

longitudinal bar of column: SD390, hoop: SD345, longitudinal and transverse bar of wall: SD345

(b) Independent columns section

building type	floor	Fc (N/mm²)	column			
			section	longitudinal bar		hoop
				X-dir	Y-dir	
14F12	12F	27	800×800	5-D29	2-D29, 3-D19	6-D10@200
14F07	7F	27	1000×1050	7-D29	2-D29, 3-D19	8-D10@200
14F03	3F	30	1050×1050	7-D29	2-D29, 3-D19	9-D10@100
14F01	1F	33	1200×1200	10-D29	9-D29	12-D10@100

longitudinal bar: SD390, hoop: SD345

(c) Columns section of 12-story building

floor	mark	Fc (N/mm²)	section	longitudinal bar			hoop
				X-dir	Y-dir	center	
9F-12F	C1	24	850×850	5-D29	5-D29	0	2-D13@100
	C2	24	850×850	5-D29	5-D29	0	2-D13@100
5F-8F	C1	30	850×850	5-D32	5-D32	0	2-D13@100
	C2	30	850×850	5-D32	5-D32	0	2-D13@100
2F-4F	C1	36	850×850	6-D35	6-D35	0	3-D13@100
	C2	36	850×850	5-D35	5-D35	8-D35	3-D13@100
1F	C1	36	850×850	6-D35	6-D35	0	3-D13@100
	C2	36	850×850	6-D35	6-D35	8-D35	3-D13@100

longitudinal bar: SD390, hoop: SD345

(d) Walls section of 12-story building

floor	Fc (N/mm²)	tickness	longitudinal bar transverse bar
9F-12F	24	300	D13@200Double
5F,7F,8F	30	300	D13@200Double
1F-4F	36	300	D13@200Double

longitudinal and transverse bar: SD295A

(e) Beams section of 12-story building

floor	Fc (N/mm²)	section	longitudinal bar			stirrup
			–	outside	inside	
RF	24	500×800	top	4-D25	1-D25	3-D13@150
			bottom	4-D25	–	
12F	24	500×800	top	4-D25	2-D25	3-D13@150
			bottom	4-D25	–	
11F	24	500×800	top	4-D29	1-D29	4-D13@150
			bottom	4-D29	1-D29	
10F	24	500×800	top	4-D29	2-D29	4-D13@150
			bottom	4-D29	1-D29	
8F,9F	30	500×800	top	4-D29	3-D29	4-D13@150
			bottom	4-D29	2-D29	
6F,7F	30	500×800	top	4-D32	4-D32	4-D13@150
			bottom	4-D32	2-D32	
5F	36	500×800	top	4-D32	4-D32	4-D13@150
			bottom	4-D32	2-D32	
2F-4F	36	500×800	top	4-D35	4-D35	4-D13@150
			bottom	4-D35	3-D35	
1F	36	500×3000	top	8-D29	4-D29	4-D16@200
			bottom	8-D29	3-D35	

longitudinal bar: SD345(1F,12F,RF), SD390(2F-11F), stirrup: SD345

3. EARTHQUAKE RESPONSE CHARACTERISTICS OF ESDOF SYSTEM

Figure 2 shows the relationship between the first mode spectral acceleration and the representative displacement. The broken lines in Figure 2 indicate the static reduction result for the first mode derived by Eqns. (5a) and (5b).

$$ {}_1S_a = \frac{\sum_{i=1}^{N} {}_1P_i \cdot {}_1\delta_i}{\sum_{i=1}^{N} m_i \cdot {}_1\delta_i} \qquad {}_1S_d = \frac{\sum_{i=1}^{N} m_i \cdot {}_1\delta_i^2}{\sum_{i=1}^{N} m_i \cdot {}_1\delta_i} \tag{5a, 5b} $$

Where ${}_1\delta_i$ is the relative displacement of the i th story with respect to the first story floor position, and ${}_1P_i$ is the horizontal load acting on the i th story. On the other hand, the black lines and the gray lines indicate the dynamic reduction result for the first mode derived by Eqns. (6a) and (6b). The black lines means the result before maximum response and the gray lines means the result after maximum response.

$$ {}_1S_a(t) = \frac{\sum_{i=1}^{N} P_i(t) \cdot {}_1\delta_i(t)}{\sum_{i=1}^{N} m_i \cdot {}_1\delta_i(t)} \qquad {}_1S_d(t) = \frac{\sum_{i=1}^{N} m_i \cdot {}_1\beta \cdot {}_1u_i \cdot \delta_i(t)}{\sum_{i=1}^{N} m_i \cdot {}_1\beta \cdot {}_1u_i} \tag{6a, 6b} $$

$$ {}_1\beta \cdot {}_1u_i = \frac{\sum_{i=1}^{N} m_i \cdot {}_1\delta_i}{\sum_{i=1}^{N} m_i \cdot {}_1\delta_i^2} \cdot {}_1\delta_i \tag{7} $$

Where $P_i(t)$ is the horizontal load acting on the i th story at time t, $\delta_i(t)$ is the relative displacement of the i th story at time t with respect to the first story floor position, and ${}_1\delta_i(t)$ is first mode component of $\delta_i(t)$ (i.e., ${}_1\delta_i(t) = {}_1\beta \cdot {}_1u_i \cdot {}_1S_d(t)$). The first mode participation vector ${}_1\beta \cdot {}_1u_i$ was calculated by Eqn. (7). Since at first the ESDOF system has not been obtained yet, ${}_1\beta \cdot {}_1u_i$ at the load step of the MAP analysis results corresponding to the peak deformation of an arbitrary story in the multi degree of freedom (MDOF) system is assumed, and reduction is carried out. Therefore, the same steps are repeated once or twice to determine ${}_1\beta \cdot {}_1u_i$ through trial and error.

As shown in figure 2, it is found that the points of maximum deformation (black circle in fig. 2) and the points of maximum deformation experienced up to each point in time (white circle in fig. 2) on the dynamic reduction result of each buildings are almost on the static reduction result regardless of the location of the soft story. Therefore, the tendency in which the static reduction result for the first mode closely corresponds to the points of maximum

deformation and the points of maximum deformation experienced up to each point in time on the dynamic reduction result regardless of the location of the soft story is found although the corresponding accuracy is less than the corresponding accuracy of the pure frame building in previous study (Kuramoto, 2006). On the other hand, it can be seen that the dynamic reduction result after maximum response has the high equivalent stiffness of steady state vibration compared with the stiffness represented by the line that connects the maximum point of both directions because the characteristics of the ESDOF system is influenced by the excessive plasticity of the soft story in the building with story collapse mechanism. The stiffness represented by the line that connects the maximum point of both directions declines because the maximum deformation of the ESDOF system is much different between negative direction and positive direction due to the plasticity of soft story. Moreover, the steady state vibration with residual deformation is observed after maximum response. Thus, the stiffness of steady state vibration becomes large because of the influence of unloading stiffness of the columns on the collapsed story.

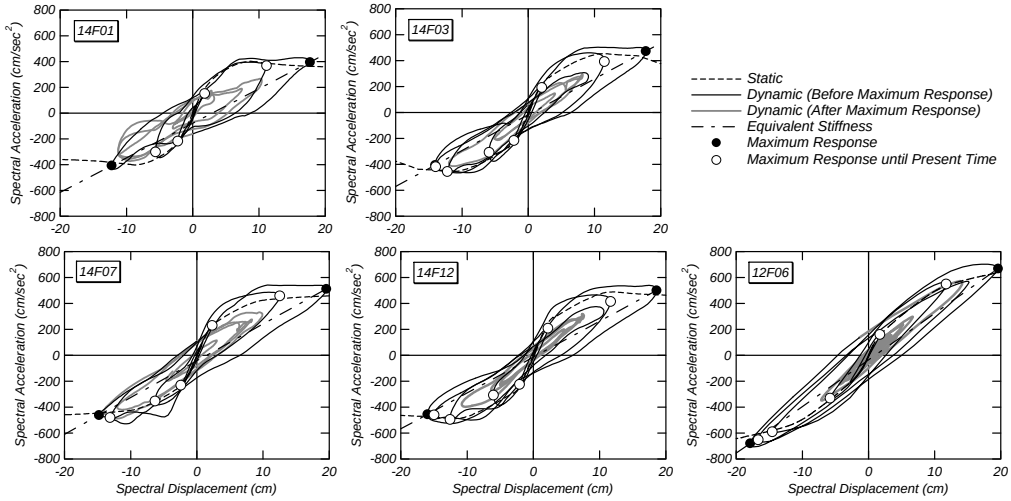

Figure 2 Relationship between the first mode spectral acceleration and the representative displacement

4. EVALUATION OF THE HIGHER MODE RESPONSE

4.1. Evaluation by Existing Equations

Figure 3 shows the evaluation results of the time history responses of the inter-story shear and drift considering the higher mode responses of the five buildings with story collapse mechanism using the Eqns. (1) and (2). Figure 3(a), (b) and (c) indicate the time history responses of the base shear and inte-story drift of the soft story of 14F01, 14F07 and 12F06 respectively. As shown in figure 3, the evaluation results of the inter-story shear are corresponded to the results of the time history analysis of every building. Thus, it is clear that Eqn. (1) can evaluate the inter-story shear of the building with story collapse mechanism accurately. On the other hand, the evaluation results of the inter-story drift are not corresponded to the results of the time history analysis of 14F01 and 14F07.

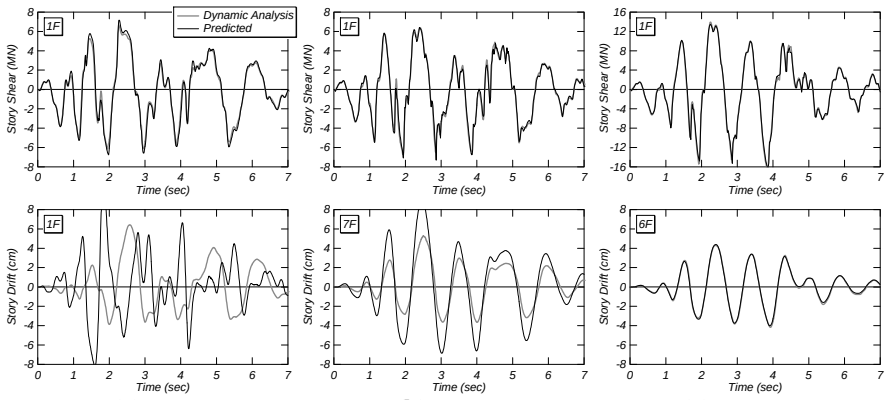

(a)14F01 (b)14F07 (c)12F06

Figure 3 Evaluation results of the time history responses of the inter-story shear and drift by Eqns. (1) and (2)

However, evaluation result has a good agreement with the time history analysis result on 12F06. Eqn. (2) can evaluate the time history of the inter-story drift as accurately as the case of the pure frame building. Therefore, it is clear that Eqn. (1) can evaluate the inter-story shear of the building with story collapse mechanism while Eqn. (2) cannot evaluate the story drift in some cases.

4.2. Examination of Equivalent Mass Ratio and Participation Vector

The equivalent mass ratio (EMR) and participation vector are examined in order to reveal the cause in which the inter-story drift is not evaluated by Eqn. (2). Figure 4 shows that the variation of the EMR of the second mode to fifth mode accompanied by the increasing of the representative displacement in the static reduction on the five buildings with story collapse mechanism and one pure frame building (12F00) which treated in previous study (Kuramoto, 2006). The el25, el50, el75 and el100 in figure 4 indicate the each input ground motion of El Centro NS. The EMR is calculated by the eigen value analysis using the equivalent stiffness which derived from the relationship between inter-story shear and inter-story drift on each step of the MAP analysis. As shown in figure 4, it can be seen that the EMR of the second mode to fifth mode decrease on 14F01, 14F03 and 14F12. On the other hand, the EMR varies considerably on 14F07 which has middle soft story, that is to say, the mode which has the maximum EMR except for the first mode changes from second mode to third mode, changes from third mode to fourth mode. Furthermore, the little variation of the EMR is observed on the 12F00 which is the pure frame building. Therefore, the variation of the EMR is small on the pure frame building because the first mode component of the inter-story drift increases almost proportionally to the elastic first mode accompanied by the progress of the plasticity. However, the inelastic first mode is different from the elastic first mode on the building with story collapse mechanism because the progress of the plasticity of the soft story is large compared with that of the other stories. Thus, the variation of the EMR is large on the building with story collapse mechanism. Regarding to the 12F06, the variation of the EMR is small because the deformation of the soft story is small in comparison with that of the other buildings with story collapse mechanism.

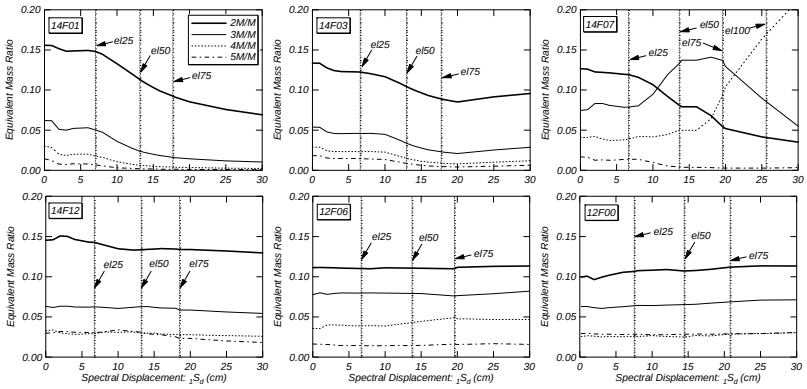

Figure 4 Variation of the equivalent mass ratio

Figure 5 shows the equivalent participation vector ($_h\beta\cdot_h u_i$) when the representative displacement of the residual ESDOF system of the dynamic reduction is maximum on 14F07, and also shows the participation vector of the second mode to fourth mode in accordance with the inelastic first mode. It is found that the $_h\beta\cdot_h u_i$ is similar to the second mode when El25 is inputted, the $_h\beta\cdot_h u_i$ is similar to the third mode when El50 and El75 are inputted, and the $_h\beta\cdot_h u_i$ is similar to the fourth mode when El100 is inputted. They are corresponded with the mode which has the maximum EMR in figure 4. As shown in figure 5, the influence of the fourth mode is relatively high because the EMR of the fourth mode increases suddenly at El75 input. As a result, $_h\beta\cdot_h u_i$ is more similar to the participation vector which combined the third mode participation vector with the fourth mode participation vector than the third mode participation vector. Figure 6 shows $_h\beta\cdot_h u_i$ and the participation vector of the second and third mode on 12F00. It is found that the elastic first mode almost same as the inelastic first mode on the pure frame building even if the input ground motion is larger. Figure 7 shows $_h\beta\cdot_h u_i$ and the participation vector of the second and third mode on 14F01, 14F03, 14F12 and 12F06 when El75 is inputted. Regarding these buildings, the EMR of the second mode is the largest and $_h\beta\cdot_h u_i$ is relatively close to the second mode constantly.

As mentioned above, it is clear that Eqn. (2) can evaluate the inter-story drift when the variation of the equivalent mass is small, that is to say, Eqn. (2) can be applied to the building which has little mode variation accompanied by

the progress of the plasticity. On the other hand, Eqn. (2) is not applicable to the building with story collapse mechanism which has large mode variation, and it is appropriate to evaluate the equivalent participation vector of the residual ESDOF system by the participation vector in which the EMR is the largest among the modes which is higher than first mode. Regarding to the evaluation of the inter-story shear, the influence of the mode variation is not effective to the inter-story shear because the arbitrary inter-story shear is the summation of the external forces acting on stories which are higher than the arbitrary story. Thus, Eqn. (1) can evaluate the inter-story shear in spite of the mode variation.

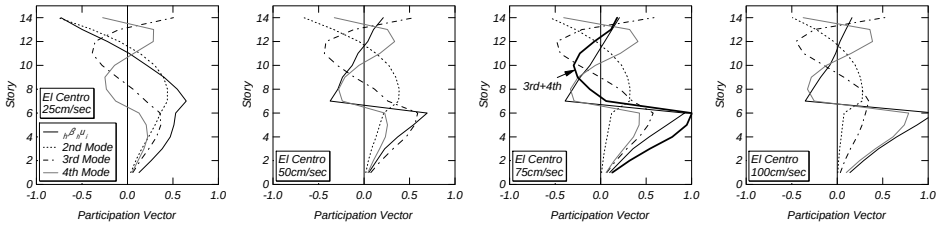

Figure 5 Comparison of the equivalent participation vector (14F07)

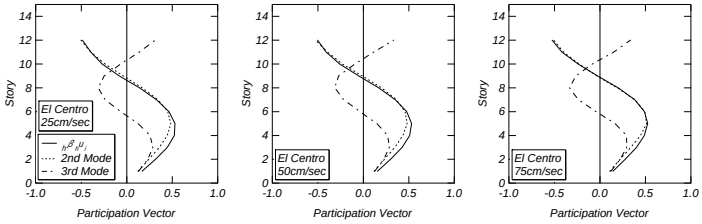

Figure 6 Comparison of the equivalent participation vector (12F00)

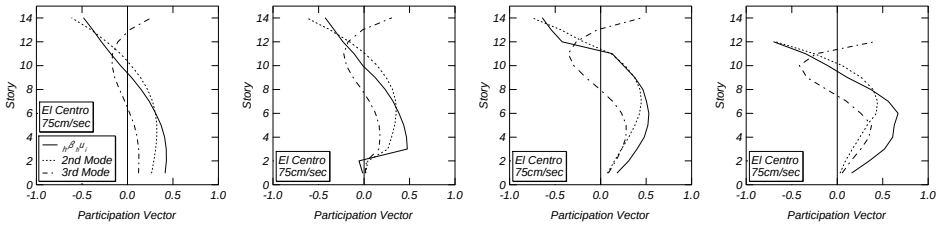

(a)14F01 (b)14F03 (c)14F12 (d)12F06

Figure 7 Comparison of the equivalent participation vector

4.3. Proposed Equations of Evaluation of Inter-story Shear and Drift

Eqns. (8) and (9) which have the participation vector of the mode with the largest EMR are obtained by the modification of the Eqns. (1) and (2). The inter-story shear can be evaluated by Eqn. (1) however Eqn. (1) should be modified to Eqn. (8) in terms of the coherence between Eqn. (8) and Eqn. (9)

$$Q_i(t) = \sum_{j=i}^{N} m_j \left\{ {}_1\beta_{\cdot 1}u_j \cdot {}_1S_a(t) + {}_{hm}\beta_{\cdot hm}u_j \cdot {}_{hm}S_a(t) - \left(1 - {}_1\beta_{\cdot 1}u_j - {}_{hm}\beta_{\cdot hm}u_j\right) \cdot \ddot{x}_0(t) \right\} \tag{8}$$

$${}_{st}\delta_i(t) = {}_1\beta\left({}_1u_i - {}_1u_{i-1}\right) {}_1S_d(t) + {}_{hm}\beta\left({}_{hm}u_i - {}_{hm}u_{i-1}\right) {}_{hm}S_d(t) \tag{9}$$

$$\sum_{i=1}^{N} m_i \cdot {}_{hm}\beta_{\cdot hm}u_i = \max\left(\sum_{i=1}^{N} m_i \cdot {}_h\beta_{\cdot h}u_i \right) \qquad (h \geq 2) \tag{10}$$

Where ${}_{hm}\beta_{\cdot hm}u_i$ is the participation vector in which the EMR is the largest among the modes which is higher than first mode considering the plasticity. ${}_{hm}S_a(t)$ and ${}_{hm}S_d(t)$ indicate the representative shear and representative displacement of the ESDOF system with respect to the mode of ${}_{hm}\beta_{\cdot hm}u_i$. They are calculated as follows.

$${}_{hm}S_a(t) = \frac{\sum_{i=1}^{N} P_i(t) \cdot {}_{hm}\delta_i(t)}{\sum_{i=1}^{N} m_i \cdot {}_{hm}\delta_i(t)} \qquad {}_{hm}S_d(t) = \frac{\sum_{i=1}^{N} m_i \cdot {}_{hm}\beta_{\cdot hm}u_i \cdot \delta_i(t)}{\sum_{i=1}^{N} m_i \cdot {}_{hm}\beta_{\cdot hm}u_i} \tag{11a, 11b}$$

$${}_{hm}\delta_i(t) = {}_{hm}\beta_{\cdot hm}u_i \cdot {}_{hm}S_d(t) \tag{12}$$

Figure 8 shows the time history response of the inter-story shear and drift of the first floor, seventh floor and fourteenth floor on 14F01 and 14F07 evaluated by Eqns. (8) and (9) when El75 is inputted. The participation vector which combined the third mode participation vector with the fourth mode participation vector is adopted to ${}_{hm}\beta\cdot{}_{hm}u_i$ on 14F07 because ${}_{h}\beta\cdot{}_{h}u_i$ is more similar to the participation vector which combined the third mode participation vector with the fourth mode participation vector than the third mode participation vector as shown in Figure 5. Eqn. (8) can evaluate the inter-story shear of 14F01 and 14F07 as accurately as Eqn. (1). Evaluation result of the inter-story drift of the soft story on 14F01 by Eqn. (9) has good agreement with the result of the dynamic analysis in comparison with the evaluation result by Eqn. (2) shown in figure 3, and the evaluation results of the other floor also have good agreement with that. Although the prediction accuracy of the inter-story drift of the soft story on 14F07 by Eqn. (9) is much better than that by Eqn. (2), Eqn. (9) still overestimates the result of inter-story drift of the dynamic analysis.

Figure 9 shows the evaluation results of the time history response of the base shear and the inter-story drift of the soft story on 14F03, 14F12 and 12F06 when El75 is inputted. It is found that the evaluation results of the base shear on every building have good agreement with the results of the time history response analysis. The evaluation

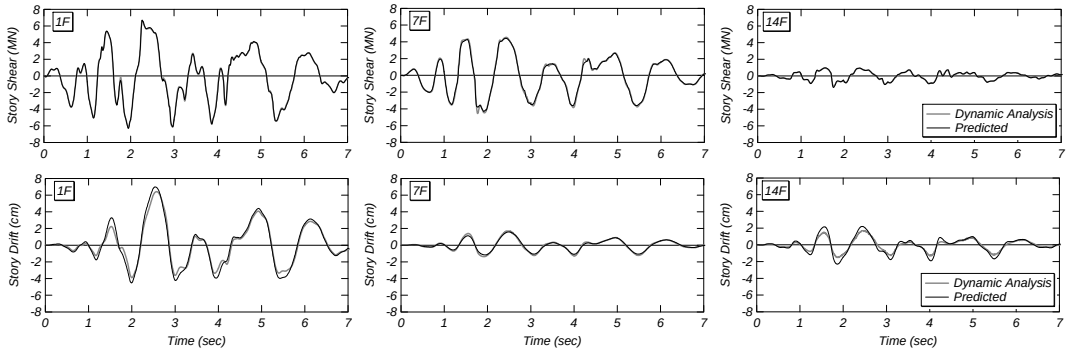

(a)14F01

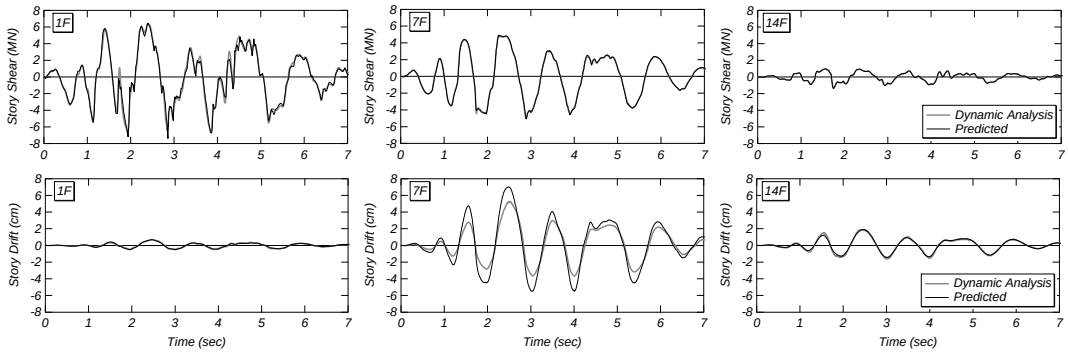

(b)14F07

Figure 8 Evaluation results of the time history responses of the inter-story shear and drift by Eqns. (8) and (9)

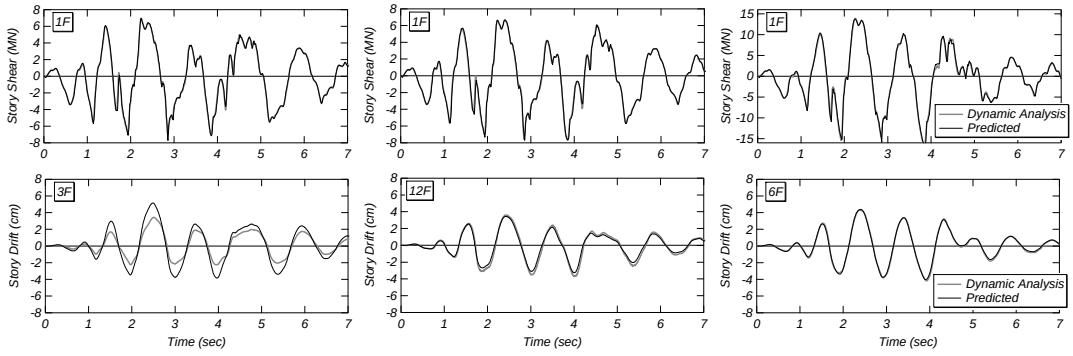

(a)14F03 (b)14F12 (c)12F06

Figure 9 Evaluation results of the time history responses of the inter-story shear and drift by Eqns. (8) and (9)

result of the inter-story drift on 12F03 exceeded the result of the time history response analysis while the evaluation results of the inter-story drift on 14F12 and 12F06 are corresponded with the results of the time history response analysis. By comparison of the evaluation accuracy on each building for the inter-story drift, the evaluation accuracies for 14F03 and 14F07 are inferior to that for 14F01, 14F12 and 12F06. As shown in Figures 5 and 7, it is caused by the less correspondence between ${}_h\beta \cdot {}_h u_i$ and the participation vector of the dominant mode among the higher modes. However, as show in figure 8 and 9, the prediction accuracy of the Eqn. (9) is relatively good, so that Eqn. (9) can evaluate almost accurately the inter-story drift of the building with story collapse mechanism.

5. CONCLUSIONS

MAP analysis and the time history response analysis for the 14-story building with soft story and 12-story building with soft story are conducted in order to consider the influence of the higher mode responses to the evaluation of the building with story collapse mechanism by CRLS. The evaluation of the time history responses of the inter-story shear and drift using the evaluation method for multi-story pure frame building proposed in previous study (Eqns. (1) and (2)) is conducted, then the applicability of Eqns. (1) and (2) is examined and the modified evaluation method (Eqns. (8) and (9)) is proposed. The findings obtained in this study may be summarized as follows.

(1) On the building with story collapse mechanism, the mode variation accompanied by the progress of the plasticity is large not only in the first mode but also in the higher mode. However, the mode variation is relatively small in the case in which the extreme story collapse is not occurred (e.g. 12F06).
(2) Eqn. (1) which evaluates the time history response of the inter-story shear is applicable to the building with story collapse mechanism because the influence of mode variation is not effective to the inter-story shear.
(3) Eqn. (2) which evaluates the time history response of the inter-story drift is applicable when the mode variation with the progress of the plasticity is small.
(4) It is appropriate to evaluate the equivalent participation vector of the residual ESDOF system by the participation vector in which the equivalent mass ratio is the largest among the modes which is higher than first mode.
(5) Eqn. (9) which considered the mode variation of the higher mode can evaluate almost accurately the inter-story drift of the building with story collapse mechanism. However, the prediction accuracy degrades when the dominant mode is changed because of the variation of the equivalent mass ratio.

REFERENCES

Freeman, S.A. (1978). Prediction of Response of Concrete Buildings to Severe Earthquake Motion, *Douglas McHenry International Symposium on Concrete and Concrete Structures* **SP-55**, American Concrete Institute, Detroit, Michigan, 589-605.

Shibata, A. and Sozen, M.A., (1976). Substitute-structure method for seismic design in R/C, *Journal of the Structural Division*, ASCE, **vol.102**, **No.ST1**, 1-18.

Kuramoto, H. (2006). Prediction of Higher Mode Shear Response for Multi-story Buildings under Earthquake Motions, *Proc. of the 8th U.S. National Conference on Earthquake Engineering*, San Francisco, California, Paper No. 1289 (CD-ROM).

Kuramoto, H. (2007). Prediction of Higher Mode Story Drift Response for Multi-story Buildings under Earthquake Motions, *Proc. of 8th Pacific Conference on Earthquake Engineering, Singapore*, Paper No.2A134 (CD-ROM).

Kuramoto, H. and K., Matsumoto. (2004). Mode-Adaptive Pushover Analysis for Multi-story RC Buildings, *Proc. of 13th World Conference on Earthquake Engineering*, Vancouver, Canada, Paper No.2500 (CD-ROM).

Takeda, T., Sozen, M.A. and Nielsen, N.N., (1970), Reinforced Concrete Response to Simulated Earthquakes, *Journal of the Structural Division*, ASCE, **vol.96**, **No.ST12**, 2557-2573.

Gu, J-H., N., Inoue and A., Shibata. (1998). Inelastic Analysis of RC Member Subjected to Seismic Loads by Using MS Model, *Journal of Structural Engineering*, AIJ, **44B**, 157-166.